Magnetotransport properties and the Fermi surface of single crystal VB_2

2008 J. Phys.: Condens. Matter 20 035209

(http://iopscience.iop.org/0953-8984/20/3/035209)

J. Phys.: Condens. Matter **20** (2008) 035209 (5pp) doi:10.1088/0953-8984/20/03/035209

Magnetotransport properties and the Fermi surface of single crystal VB_2

A B Karki[1], D P Gautreaux[2], J Y Chan[2], N Harrison[3], D A Browne[1], R G Goodrich[1] and D P Young[1,4]

[1] Department of Physics and Astronomy, Louisiana State University, Baton Rouge, LA 70803, USA
[2] Department of Chemistry, Louisiana State University, Baton Rouge, LA 70803, USA
[3] National High Magnetic Field Laboratory, Los Alamos National Laboratory, Los Alamos, NM 87545, USA

E-mail: dyoung@rouge.phys.lsu.edu

Received 2 September 2007, in final form 9 November 2007
Published 17 December 2007
Online at stacks.iop.org/JPhysCM/20/035209

Abstract

We report the results of magnetotransport and de Haas–van Alphen (dHvA) measurements on high quality single crystals of VB_2 grown from a molten aluminum flux. In addition, we compare these results to energy band calculations. At low temperature the magnetoresistance of VB_2 is very large (∼1100%) and is found to be extremely sensitive to sample quality (RRR value). A large anisotropy in the magnetoresistance is observed. For the field applied along the *a*-axis, the magnetoresistance increases as the square of the field without saturation, consistent with the presence of open orbits. The field dependence of the magnetoresistance for the field applied along the *c*-axis is much weaker.

1. Introduction

Transition metal diborides with the simple AlB_2 structure type have been studied since the late 1940s. These early works focused primarily on the mechanical properties of these materials, because they have high microhardnesses and are very refractory, making them useful in high temperature applications [1]. The transition metal diborides are also of interest, since they form an isostructural series that runs from Sc through Fe in the first row of transition metals. Thus, these materials offer a rare opportunity to study the variation in electronic properties within this single structure type as one moves along the series.

More recently, however, the diborides are being reinvestigated due to the discovery of superconductivity near 40 K in MgB_2 [2]. MgB_2 and the transition metal diborides of Cr, Fe, Mn, Mo, Nb, Sc, Ta, Ti, V, W, Y, and Zr all form in the simple AlB_2 structure type. With the exception of Nb, none of the other transition metal diborides have been confirmed as superconductors [3]. If VB_2 does superconduct, then it's predicted to do so at temperatures <1 K [4].

Here we report the magnetotransport properties of single crystals of VB_2. The high quality of the samples has allowed us to experimentally determine the Fermi surface of VB_2 and compare it to theoretical calculations. An unusually large magnetoresistance is observed at low temperature in the highest quality crystals.

2. Experiment

The single crystals of VB_2 were synthesized by a metallic flux technique using molten aluminum at high temperature. This is a standard synthesis method for refractory borides. The starting materials consisted of V turnings (99.7% CERAC, INC.), amorphous B powder (99.99% Alfa AESAR), and Al shot (99.999% Alfa AESAR). Stoichiometric amounts of V and B were placed in an aluminum oxide crucible with excess Al shot. The molar ratio of the starting elements V:B:Al was 1:2:190. The crucible was then placed at the center of a vertical tube furnace and heated in an inert atmosphere of flowing ultra high purity argon gas. The furnace was heated from room temperature to 1400 °C in 6 h and maintained at that temperature for 10 h, followed by cooling to 1000 °C at a rate of 50 °C h^{-1}. At this point the furnace was shut off and allowed to cool to room temperature. The single crystals were extracted from the solid aluminum by etching it away with a hot solution of NaOH. The crystals were collected and

[4] Author to whom any correspondence should be addressed.

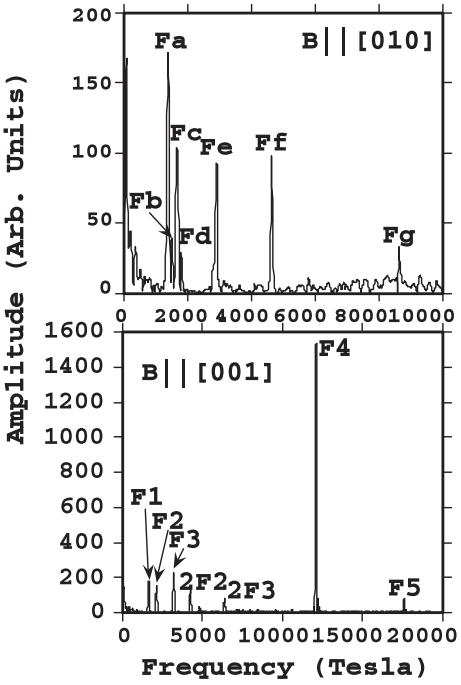

Figure 1. FFTs of the dHvA data for $B \parallel [010]$ and $B \parallel [001]$. The symbols are the names assigned to each fundamental frequency and some harmonics.

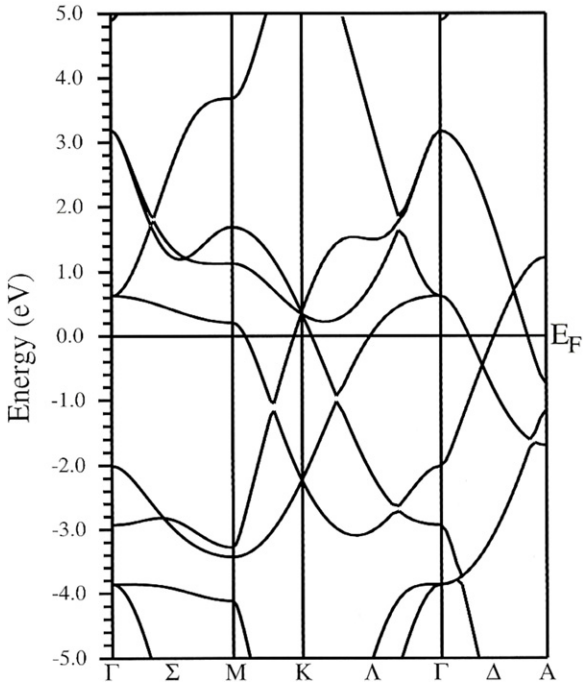

Figure 2. The calculated electronic band structure of VB_2 in the vicinity of the Fermi level. Designations on the horizontal axis represent high symmetry directions in the hexagonal Brillouin zone.

their surfaces cleaned by etching in very dilute nitric acid. Finally, the crystals were washed, rinsed with ethanol, and dried. The crystals grew both as rods and flat plates, with typical dimensions on the order of 1 mm × 1 mm × 4 mm. The AlB_2-type structure of VB_2 was verified by single crystal x-ray diffraction. A small crystal fragment was glued to a glass fiber and mounted on the goniometer of a Nonius Kappa CCD diffractometer equipped with Mo Kα radiation (λ = 0.710 73 Å). Data were collected at 293 and 90 K.

A polycrystalline sample of VB_2 was also made by arc melting stoichiometric amounts of V and B on a water-cooled copper hearth under ultra high purity argon gas. The sample was then wrapped in Ta foil, sealed in a quartz tube under vacuum, and annealed for 5 days at 900 °C. Single phase VB_2 was confirmed by powder x-ray diffraction.

The electrical resistivity and magnetoresistance were measured using a standard 4-probe technique, in which small diameter Pt wires were attached to the sample using a conductive epoxy (Epotek H20E). Data were collected from 1.8 to 290 K and in magnetic fields up to 9 T using a Quantum Design PPMS system.

Single crystal samples of approximate dimensions 0.2 mm×0.2 mm×0.2 mm were used for dHvA measurements. Two different samples, one with the applied magnetic field along the [001] axis and one with the field parallel to the [010] axis were measured. The measurements were made using pulsed magnetic fields extending to 55 T at the National High Magnetic Field Laboratory, Los Alamos, New Mexico. Measurements were taken in the temperature range from 450 mK to 6 K using a plastic [3] He refrigerator.

3. Results and discussion

Typical fast Fourier transforms (FFTs) of the dHvA data for $B \parallel [001]$ and $B \parallel [010]$ giving the frequencies reported here are shown in figure 1. The frequencies of the dHvA oscillations are proportional to extremal areas of the Fermi surface perpendicular to the applied field direction. From the temperature dependence of the amplitudes of the FFT peaks, the effective masses were obtained [5]. Table 1 gives a summary of the measured frequencies and effective masses for each field orientation. We suspect that the 8625 T frequency, which is broad and indistinct, is associated with the second zone orbit of Al that is left over from the crystal growth.

The band structure of VB_2 was calculated using the WIEN2K full potential LAPW band package, [6] using the GGA exchange correlation potential [7]. The muffin tin radii were taken as 2.4 au for V and 1.62 au for B. The cutoff in the LAPW basis was varied from G_{max} of 2.5 $(au)^{-1}$ (170 plane waves) to 3.75 $(au)^{-1}$ (468 plane waves). The mesh of k-points in the irreducible wedge of the Brillouin zone included 512 points, giving a total of 10 000 points in the full Brillouin zone. To improve the convergence of the V d bands, local d orbitals were added at 0.9 Ryd (about 2 eV above the Fermi level). Calculations were performed using both the room temperature lattice constants and also the lattice constants measured at 90 K. Also, a minimization was performed to find the theoretical equilibrium lattice constants. Finally, we used room temperature lattice constants measured by Loennburg *et al* [8].

The results of these calculations are presented in figure 2 for the bands and figure 3 for the density of states. The states

Table 1. Measured dHvA frequencies and effective masses for single crystalline VB_2. The left side of the table corresponds to $B \parallel [001]$, and the right side corresponds to $B \parallel [010]$.

$B \parallel [001]$			$B \parallel [010]$		
	Freq. (T)	$m^* = m/m_0$		Freq. (T)	$m^* = m/m_0$
F1	1 668	0.58 ± 0.01	Fa	1404	0.53 ± 0.02
F2	2 127	0.380 ± 0.008	Fb	1510	0.33 ± 0.04
F3	3 200	0.491 ± 0.007	Fc	1662	0.36 ± 0.02
F4	12 105	1.10 ± 0.04	Fd	1819	0.44 ± 0.05
F5	17 613	1.7 ± 0.3	Fe	2898	0.74 ± 0.05
			Ff	4639	1.00 ± 0.14
			Fg	8625	1.05 ± 0.10

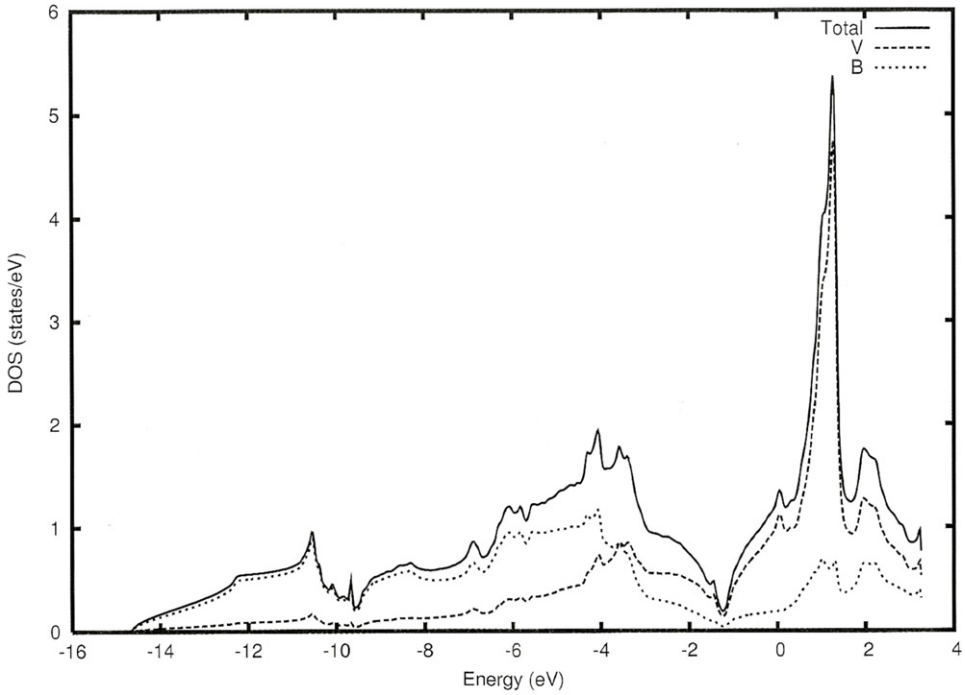

Figure 3. The calculated total (solid line) and partial density of states for VB_2. The large peak in the density of states near the Fermi level is almost entirely composed of V d orbitals.

at the Fermi level are derived almost entirely from the d bands of vanadium, in contrast to the case in MgB_2, where the high energy part of the valence band is made up predominantly of boron 2p states [9]. Because of these relatively flat bands near the Fermi level, some of the Fermi surface areas change substantially (15%) as the lattice constants are changed by less than 1%. For example, the empty band just above the Fermi level from Gamma to M reaches the M-point just above the Fermi level, resulting in a small hole pocket there. Changes in the lattice constants by less than 1% can result in this pocket of holes vanishing. Thus, while most of the overall topology of the Fermi surface agrees among the four calculations, the theoretical predictions of the Fermi surface shape are not in excellent agreement with the measured values. The results that we show are very similar to other calculations [4, 10, 11] done on VB_2 using other basis sets, but those authors did not note the sensitivity of their Fermi surfaces to changes in lattice constant. The sensitivity to lattice constant suggests that pressure studies in this material might reveal transitions associated with the appearance or disappearance of some sheets of the Fermi surface.

The main section of the Fermi surface is displayed in figure 4(a) using the lattice constants measured at 90 K. It resembles a six-sided tree trunk. The other sections are nearly spherical pockets of electron states (figure 4(b)). One pair is located at $q_z = \pm 0.16\pi/c$, and the other two are located on the upper face of the Brillouin zone at $q_z = \pi/c$.

For magnetic fields aligned along the (001) direction, we find two extremal orbits in the $q_z = 0$ plane, surrounding the K-point. The smaller one is a hole orbit, and the larger one is an electron orbit. This larger one gives rise to the high frequency dHvA signal seen in the experiment. In addition to these orbits, there is an electron orbit at $q_z = \pm 0.16\pi/c$, a hole orbit derived from the same band that gives rise to the trunk-like piece of the Fermi surface at $q_z = \pi/c$, and an electron orbit at $q_z = \pi/c$ (figure 4(b)). The areas and frequencies found for these surfaces for each of the four calculations are listed in table 2.

Table 2. Calculated frequencies with magnetic field in different directions for experimentally determined lattice constants of VB_2 (columns 1, 2, and 4) and for the theoretically determined equilibrium lattice constants (column 3).

	90K lattice constants	Room temperature lattice constants	Theoretical equilibrium	Lonnburg
a (Å)	2.998	3.000	3.006	2.998
c (Å)	3.044	3.062	2.997	3.055
Field along 001				
Large orbit at K (T)	15 900	16 400	14 100	16 500
Small orbit at K (T)	207	225	290	111
Large orbit on trunk at π/c (T)	10 400	10 400	9300	11 470
Larger ellipsoid at π/c (T)	1980	1970	1820	2270
Smaller ellipsoid at π/c (T)	1510	1520	1400	1710
Sphere at $q_z = 0.45\pi/c$ (T)	1100	1250	790	1590
Field along 100/210				
Larger ellipsoid at π/c (T)	1640	1670	1440	1920
Smaller ellipsoid at π/c (T)	1340	1360	1190	1550
Sphere at $q_z = 0.45\pi/c$ (T)	920	1150	700	1460
Interior below trunk (100 only) (T)	5000	4750	5540	4100
'Roots' on face (100 only) (T)	2400	2550	2100	2890
Around outside of trunk (210 only) (T)	20 500	21 500	18 000	24 300

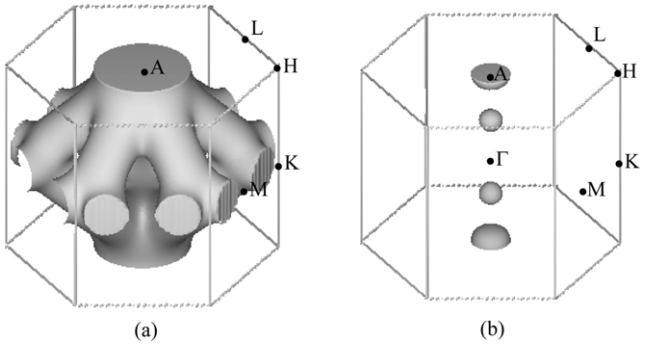

Figure 4. The Fermi surface of VB_2. The main section (a) resembles a six-sided tree trunk. The other sections (b) are nearly spherical pockets of electron states which are obscured by the larger Fermi surface. One pair is located at $q_z = \pm 0.45\pi/c$, and the other two (one is omitted for clarity) are located on the upper face of the Brillouin zone at $q_z = \pi/c$ (at the A-point).

From figure 4(a) it is also apparent that the tubular structure on each side of the main part of the Fermi surface will give a dHvA signal at a field about 30° above and below the ab-plane and that the frequency dependence will vary as $1/\cos\theta$, where θ is the angle measured form the tube direction. This would confirm the general features of the Fermi surface that we are seeing.

The electrical resistivity of the VB_2 single crystals was measured from 290 K down to 1.8 K (not shown). The samples were metallic, and no superconductivity was observed. The residual resistivity ratio (RRR), which is defined as RRR $= \rho$ (290 K)$/\rho$ (1.8 K) varied from crystal to crystal, with typical values falling in the range of 100–150. Samples with RRR values as high as 258 were measured, and indicate excellent sample quality.

The magnetotransport properties of VB_2 are shown in figure 5. All the transport properties were made with the current parallel to the c-axis. The magnetoresistance (MR), which is defined as MR $= [(\rho(H) - \rho(0))/\rho(0)]$, plotted versus applied magnetic field is shown at different temperatures for a single crystal of VB_2 with a RRR value of 258. At all temperatures, the magnetoresistance increases with applied field and decreases with increasing temperature. At 3 K (right axis, figure 5) the magnetoresistance at 9 T is unusually large (∼1100%) and shows no tendency toward saturation. In general, classical theory predicts that the high field transverse magnetoresistance of a normal metal depends on the Fermi surface topology [13]. The magnetoresistance should saturate at high fields for closed orbits, or continue to increase as H^2 for open orbits. The solid lines in the main panel of figure 5 are quadratic fits to the data, showing that the MR does indeed increase as H^2 up to a field of 9 T, suggesting open orbits for the field applied along the a-axis.

The lower inset in figure 5 demonstrates the large anisotropy in the magnetotransport for a single crystal of VB_2 at 3 K. The quadratic field dependence observed in the MR for $H \parallel a$ is not observed for $H \parallel c$, but a much weaker field dependence occurs. This is also consistent with the *calculated* Fermi surface. The calculation indicates that for a field in the [100] direction, an open orbit exists that runs along the trunk of the Fermi surface shown in figure 4. For the [110], or b-direction, this open orbit is absent. Any disorder in the sample that resulted in 30° twins would produce a mixture of open and closed orbits for electrons moving along the trunk. This may well explain the large, unsaturated magnetoresistance observed in these samples.

The upper inset of figure 5 demonstrates the sensitivity of the MR to the quality of the samples. Generally, a larger RRR value indicates higher crystal quality. Here, the value of the MR measured at 3 K and 9 T is plotted versus the RRR value for several different single crystals of VB_2. The size of the MR increases dramatically with the RRR value. The solid line in the inset represents the following fit to the data: MR $= \alpha$ (RRR) [2], where $\alpha = 1.65 \times 10^{-4}$.

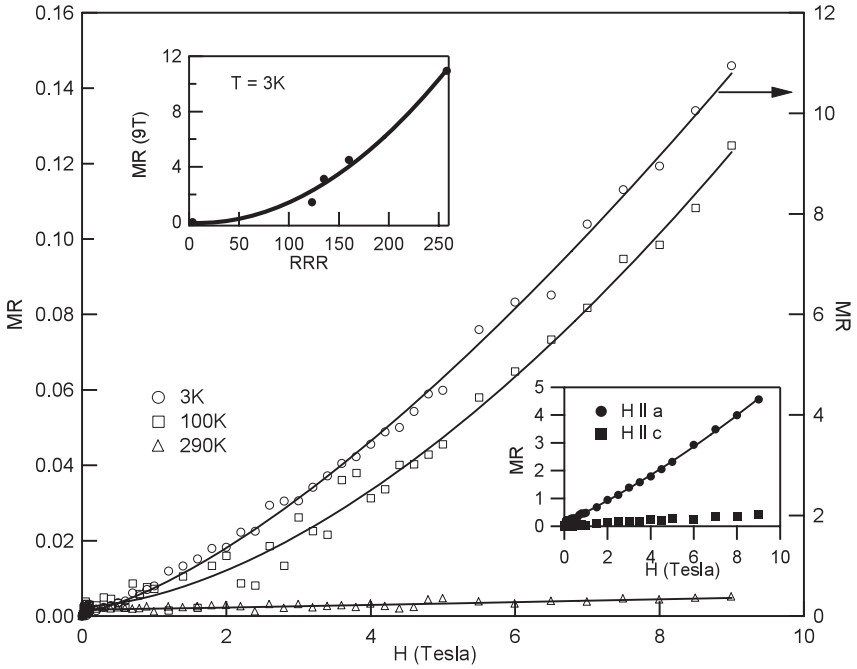

Figure 5. The magnetic field dependence of the isothermal magnetoresistance at three different temperatures for the VB_2 single crystal with RRR = 258 and $H \parallel a$ and $I \parallel c$. The right axis corresponds to the 3-K data. The solid lines in the main panel and the two insets are fits proportional to H^2. Upper inset: magnetoresistance at 3 K and 9 T plotted versus the RRR value for different single crystals of VB_2. Lower inset: shows the large anisotropy in the magnetoresistance of a single crystal of VB_2 at 3 K for the field applied along the a- and c-axes.

In many metals the MR behavior is known to follow Kohler's rule i.e. $\Delta\rho/\rho(0) = f(H/\rho(0))$ [12]. Attempts to show that Kohler's rule is obeyed were inconclusive due to the scatter in the data at low fields. However, the correlation that exists between the MR and the RRR values suggest this to be the case. Based on Kohler's rule, the isothermal magnetoresistance should obey the following: $\Delta\rho/\rho_0 \sim (H/\rho_0)^2$. For metals, $\rho(0) \sim (1/l)$, where l is the mean free path. Thus, the magnetoresistance should follow: $\Delta\rho/\rho_0 \sim (Hl)^2$. The RRR value is proportional to the mean free path (l) at low temperatures, so that $\Delta\rho/\rho_0 \sim (\mathrm{RRR})^2$, which is the behavior we observe (figure 5 inset).

4. Conclusion

We have succeeded in growing very high quality single crystals of VB_2 and experimentally determined the Fermi surface via dHvA measurements. Some of the crystals had a RRR value in excess of 250. Electronic structure calculations confirm that the density of states near the Fermi surface is dominated by vanadium d orbitals, unlike the case of MgB_2. Magnetotransport measurements show a very large magnetoresistance at low temperatures which scales quadratically with the residual resistivity ratio. Given the large sensitivity of the Fermi surface topology to the lattice constants, we are motivated in future work to investigate the magnetotransport properties of VB_2 under pressure.

Acknowledgments

Work conducted at the National High Magnetic Field Laboratory was supported by the National Science Foundation (NSF) and the State of Florida. Both RGG and DPY gratefully acknowledge support from the NSF under Grant No. DMR 04-49022 (DPY). JYC acknowledges support from the NSF under Grant No. DMR 02-37664 and from the Alfred P Sloan Foundation.

References

[1] Vasilos T and Rhodes W H 1973 *Am. Ceram. Soc. Bull.* **52** 643
Nakano K, Matsubara H and Imura T 1976 *J. Less-Common Met.* **47** 259–64
Lisy F, Abada A and Vedula K 1987 *J. Met.* **39** A61
[2] Nagamatsu J, Nakagawa N, Muranaka T, Zenitani Y and Akimitsu J 2001 *Nature* **410** 63–4
[3] Buzea C and Yamashita T 2001 *Supercond. Sci. Technol.* **14** R115
[4] Mahmud S T, Islam A and Islam F N 2004 *J. Phys.: Condens. Matter* **16** 2335–44
[5] See, for example Shoenberg D 1984 *Magnetic Oscillations in Metals* (Cambridge: Cambridge University Press)
[6] Blaha P, Schwarz K, Madsen G K H, Kvasnicka D and Luitz J 2001 *WIEN2K, An Augmented-Plane-Wave + Local Orbitals Program for Calculating Crystal Properties* (Vienna: Karlheinz Schwarz, Technical University of Wien)
[7] Perdew J P, Burke K and Ernzerhof M 1966 *Phys. Rev. Lett.* **77** 3865
[8] Lonnberg B 1988 *J. Less-Common Met.* **141** 145
[9] Medvedeva N I, Ivanovskii A L, Medvedeva J E and Freeman A J 2001 *Phys. Rev.* B **64** 020502(R)
[10] Vajeeston P, Ravindran P, Ravi C and Asokamani R 2001 *Phys. Rev.* B **63** 045115
[11] Shein I R and Ivanovskii A L 2002 *Phys. Solid. State* **44** 1833–9
[12] Lifshits I M and Peschanskii V G 1959 *Sov. Phys.—JETP* **8** 875
[13] See, for example Abrikosov A A 1988 *Fundamentals of the Theory of Metals* (Amsterdam: North-Holland)